Gas-Phase ^{1}H NMR Studies of Internal Rotation Activation Energies and Conformer Stabilities of Asymmetric *N,N*-Disubstituted Formamides and Trifluoroacetamides

A. N. Taha, S. M. Neugebauer Crawford, and N. S. True*

Chemistry Department, University of California, Davis, California 95616

Received: October 22, 1997

Activation parameters and conformational stabilities characterizing the internal rotation about the peptide bond in a series of *N,N*-asymmetric dialkylformamides ($HCONR_1R_2$: $R_1 = CH_3$, R_2 = propyl, butyl, and isopropyl) and *N,N*-asymmetric dialkyltrifluoroacetamides ($F_3CCONR_1R_2$: $R_1 = CH_3$, R_2 = propyl, butyl, and isopropyl) are determined from temperature-dependent gas-phase ^{1}H NMR spectra. Conformer free energy differences, ΔG^0_{298}(syn−anti), in cal mol^{-1}, and activation free energies, $\Delta G^{\ddagger}_{298}$, in kcal mol^{-1} , for the formamides are −83(14)/19.4(0.1) for R_2 = propyl, −80(14)/19.3(0.1) for R_2 = butyl, and −91(13)/19.1(0.1) for R_2 = isopropyl and for the trifluoroacetamides 178(24) /16.8(0.1) for R_2 = propyl, 191(53)/16.6(0.1) for R_2 = butyl, and 218(29)/16.3(0.1) for R_2 = isopropyl. The preferred conformer in both the gas and liquid phases has the *N*-methyl group syn to the carbonyl oxygen in the formamide systems and the *N*-methyl group anti to the carbonyl oxygen in the trifluoroacetamides. The gas-phase results are compared to liquid-phase values.

Introduction

The importance of syn/anti isomerization about the peptide bond in the biological function of enzymes and proteins is well-known.[1,2] The stability of secondary and tertiary structures is derived partly from the planar structure and relatively high barrier to rotation about the C−N bond. The high barrier to rotation about the C−N bond in amides is characterized by the simple resonance model where the contribution of partial double bond character from resonance form **II** to the ground state leads to subsequent inhibition of free C−N bond rotation. In the planar ground state, the nitrogen atom, in an attempt to minimize the energy of its lone pair electrons, interacts with an electron-deficient carbonyl carbon atom.[3] Effects of substitution at the carbonyl carbon have been more extensively studied than nitrogen substituent effects and are quite successfully characterized by the simple resonance model.[4] It has been shown that carbonyl substituents larger than Y = H lower the barrier to internal rotation through destabilization of the planar ground state due to Y−R crowding.[5] Effects of electron-withdrawing and -donating substituents are described in terms of their stabilization and destabilization of the transition-state structure.[5] The present study focuses on investigating the rotational barrier dependence on substitution at the amide nitrogen in asymmetrically substituted amides.

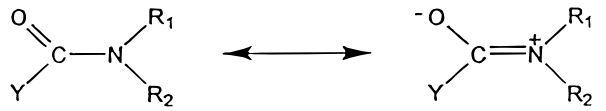

I II

Asymmetrically substituted amides are of great interest because they display conformer population differences. Many theoretical investigations have focused on these differences in attempts to describe the contribution of each conformer in stable protein structures.[6−11] A previous study by LeMaster and True[12] reported that internal rotational barriers in *N,N*-symmetric disubstituted formamides decrease with increasing size of alkyl substituents on the amide nitrogen. Similar results were obtained for *N,N*-symmetric disubstituted trifluoroacetamides.[13] Again, rotational barriers were observed to decrease with increasing alkyl substituent size. In 1995, Suarez and True[14] presented the first systematic study of rotational barriers in the gas phase of asymmetrically substituted amides. Their studies of gas- and solution-phase *N*-ethyl-*N*-methylformamide, *N*-ethyl-*N*-methyltrifluoroacetamide, and *N*-ethyl-*N*-methylacetamide found that, as with the disubstituted systems, the rotational barrier decreases with increasing substituent bulk, but to a lesser extent in the trifluoroacetamides where electronegativity differences dominate. They also report liquid rotational barriers which are ≈1−2 kcal mol^{-1} greater than the gas-phase values.

Variable-temperature NMR methods allow for the elucidation of the temperature dependence of interconversion rate constants and conformer populations to yield a complete set of kinetic and thermodynamic parameters. This method has been widely used in the study of conformational stability and exchange kinetics in liquid amides.[4,5,15] Gas-phase experimental data allow for a more direct analysis of trends, reveal intrinsic molecular characteristics, and can be used directly to test the reliability of theoretical calculations, which generally examine isolated molecules. We present gas-phase kinetic parameters obtained from exchange broadened variable temperature NMR studies for a series of asymmetrically substituted formamides and trifluoroacetamides and compare them to the solution-phase values.

This study reports the Gibbs free energy differences, $\Delta G^{\ddagger}$ and $\Delta G°$, characterizing the hindered rotation about the C−N bond in gaseous and solution-phase systems of *N*-methyl-*N*-propylformamide (MPF), *N*-butyl-*N*-methylformamide (MBF), *N*-isopropyl-*N*-methylformamide (MIF), *N*-methyl-*N*-propyltrifluoroacetamide (MPTFA), *N*-butyl-*N*-methyltrifluoroacetamide (MBTFA), and *N*-isopropyl-*N*-methyltrifluoroacetamide (MITFA). This is the first gas-phase study of these systems. The solution-phase measurements yield information about the stabilizing and destabilizing effects of solvent perturbations on the peptide bond torsional barrier. It has been well established that amide self-association, solvent−amide association, solvent polarity, and increased internal pressure due to phase affect the

S1089-5639(97)03408-7 CCC: $15.00
Published on Web 01/30/1998

reaction rate.[13] It has also been suggested that $\Delta G^{\ddagger}$ increases with high amide concentration (>15 mol %) in solution systems due to amide aggregation.[8] We have, therefore, examined 1 mol % amide solutions in the present study.

Experimental Section

Synthesis of Asymmetric Formamides. All asymmetric formamides were prepared by aminolysis of ethyl formate with the corresponding amine: *N*-methylpropylamine, *N*-methylisopropylamine, and *N*-methylbutylamine. The addition of ethyl formate (0.2 mol) to the amine (0.1 mol) in ethanol was carried out in an ice−salt bath with constant stirring and then allowed to reach room temperature. The reaction mixture was subsequently refluxed for 1−3 h and then stirred overnight. Fractional distillation yielded the amide product.

Synthesis of Asymmetric Trifluoroacetamides. All asymmetric trifluoroacetamides were prepared by slow addition of a molar excess of trifluoroacetic anhydride to the corresponding amine at 0 °C. The resulting reaction mixture was washed with saturated aqueous sodium bicarbonate and extracted into diethyl ether. The ether was removed to yield the trifluoroamide product.

All reagents were purchased from Aldrich Chemical Co. and used without further purification. All amide products were characterized by ^{1}H NMR spectroscopy.

Sample Preparation. Gas-phase NMR samples were prepared in restricted volume NMR tubes constructed from 3 cm long sections of Wilmad high-precision 12 mm coaxial inserts. The short tubes were inserted into longer 12 mm tubes for introduction into the probe. The shorter tubes confined the sample and reduced the temperature gradient within the active volume. Atmospheric pressure samples were prepared by deposition of a small drop of the amide in the bottom of the sample tube. A small drop of tetramethylsilane (frequency and resolution reference) was also added to the slightly cooled 3 cm insert tubes prior to torch sealing. The amide gas equilibrates at its vapor pressure which increases as the probe temperature increases. This allows for the sample vapor pressure and thus the NMR signal to increase with temperature. Samples were run from low to high temperature to avoid condensation on the walls of the insert tube. Amide internal rotation rate constants are not pressure dependent at pressures between a few Torr and several atmospheres.[16]

Solution-phase samples were prepared in 5 mm o.d. Wilmad NMR tubes and contained 1 mol % amide in tetrachloroethane-d_2 (TClE, Aldrich). TClE, which boils at 146 °C, was used because of the relatively high temperature of the exchange regions for MBF, MPF, and MIF and its relative nonpolarity. All liquid samples also contained a drop of TMS as a frequency and resolution reference.

Spectroscopic Measurements. Gas-phase ^{1}H NMR spectra were acquired on a wide-bore GE NT-300 spectrometer (proton observation at 300.06 MHz) fitted with a Tecmag acquisition upgrade and equipped with a Bradley 12 mm proton probe. Liquid-phase ^{1}H NMR spectra were also acquired on a wide-bore GE NT-300 spectrometer (proton observation at 300.07 MHz) fitted with the Tecmag acquisition system and equipped with a Bradley 5 mm proton probe. All measurements were made on spinning samples in unlocked mode. Acquisition parameters were as follows: pulse length, 14 μs (90° flip angle); delay time, 1.3 s; and acquisition time, 1.0 s. Delay times for all liquid spectra were 5 s. No changes in the population ratios were observed for sample acquisitions with 5 and 10 s delay times for the gas and solution samples, respectively. Typically 1000−3000 transients were collected for the gaseous samples and 16 for the solution samples at each temperature and stored in 8K of memory to achieve a maximum signal-to-noise of 10:1 and 100:1 after multiplication by an exponential line broadening factor of 1 Hz. A sweep width of ±2500 Hz was employed, giving a digital resolution of 0.6 Hz/point. Temperatures were controlled with a 0.1 °C pyrometer and read after each acquisition. Temperature measurements for the gas-phase spectra were made using two copper−constantan thermocouples placed within an empty 3 cm long, 12 mm o.d. insert tube fitted within a 12 mm NMR tube. This design closely resembles the experimental sample system. Using this technique, the temperature gradient within the active volume of the probe was found to be less than 0.2 K. Samples were allowed to thermally equilibrate for at least 10 min prior to sample acquisition. Liquid temperatures were measured in the same manner, except that a single 5 mm NMR tube containing TClE and one copper−constantan thermocouple was employed.

Parameter Determination. Rate constants were calculated using the computer program DNMR5,[17] which uses an iterative nonlinear least-squares regression analysis to obtain the best fit for the experimental NMR spectra. The program was provided with anti and syn proton chemical shifts at the limit of slow exchange, coupling constants, transverse relaxation times, and the digitized NMR spectrum. The effective line width parameter was measured at slow and fast exchange for each amide. The effective line width was estimated at each temperature by assuming a linear temperature dependence. The line width of TMS at each exchange temperature was used to estimate the magnetic field inhomogeneity contribution to the line width. This factor and the exponential line broadening factor were added to the interpolated values for the effective line width to obtain a total line broadening, and thus the effective transverse relaxation time (T_2) was determined at each temperature. Rate constants in the exchange region were obtained by iterating on rate constant, spectral origin, baseline height, and baseline tilt. All other parameters were held constant.

Conformer Gibbs energy differences, $\Delta G°$, were calculated through extrapolation of $\Delta H°$ and $\Delta S°$ from the slope and intercept of $1/T$ versus ln K_{eq} according to the van't Hoff equation. The $\Delta G°$ values are reported at 298 K. The changes of the population ratios in the slow exchange region allowed for the characterization of K_{eq} as a function of temperature. All populations were determined by the average of 20 integrations. Gas-phase slow exchange population ratios, p_{syn}/p_{anti}, ranged from 1.12 to 1.06 for MPF, 1.11 to 1.08 for MBF, 1.16 to 1.10 for MIF, 0.73 to 0.78 for MPTFA, 0.73 to 0.78 for MBTFA, and 0.68 to 0.78 for MITFA.

Results

Exchange rate constants used to determine gas-phase activation parameters from exchange broadened spectra are tabulated in Table 1. Eyring plots of the gaseous rate constants are shown in Figure 1. Table 2 lists the experimental gas- and solution-phase conformer Gibbs energy differences and percentage of syn conformer for each amide system at 298 K. The experimental activation parameters for the gaseous and solution systems are given in Table 3. Conformer assignments are described below followed by results of the exchange broadened line shape analyses.

Conformational information was obtained by analysis of the slow exchange spectra for all six amide systems in both the gas and solution phases. The resolved spectra clearly show two conformational forms: syn (the *N*-methyl group syn to carbonyl

TABLE 1: Rate Constants (k) for Internal Rotation in Gaseous MPF, MBF, MIF, MPTFA, MBTFA, and MITFA as a Function of Temperature

MPF		MBF		MIF		MPTFA		MBTFA		MITFA	
T (K)	k (s^{-1})	T (K)	k (s^{-1})	T (K)	k (s^{-1})	T (K)	k (s^{-1})	T (K)	k (s^{-1})	T (K)	k (s^{-1})
338.1	2.1(0.3)	350.4	7.1(1.6)	346.8	6.6(0.5)	299.4	3.8(0.3)	300.2	5.3(0.4)	310.8	22.4(0.3)
344.4	4.1(0.3)	355.0	6.4(1.7)	351.5	9.0(0.3)	302.2	4.9(0.3)	304.0	6.9(0.4)	312.9	23.8(0.2)
346.8	6.2(0.4)	359.1	13.8(2.1)	354.6	12.0(0.2)	303.0	4.8(0.3)	305.8	8.8(0.6)	314.7	27.7(0.8)
349.8	5.4(0.2)	365.1	14.8(1.7)	356.2	14.4(0.1)	308.1	7.9(0.3)	308.2	10.5(0.3)	316.7	34.3(0.5)
353.5	8.7(0.2)	366.9	21.0(1.6)	358.7	17.0(0.0)	310.5	10.2(0.3)	310.3	10.5(0.3)	316.7	34.3(0.5)
353.8	10.7(1.3)	371.5	32.0(1.7)	362.8	21.8(0.0)	311.9	11.1(0.5)	312.7	17.2(0.5)	320.2	45.1(0.6)
356.2	12.0(0.5)	377.8	43.3(1.6)	361.7	20.9(0.0)	314.3	14.6(0.3)	314.0	18.8(0.5)	322.0	56.0(0.7)
369.0	43.4(0.6)	381.6	67.0(2.0)	364.7	29.2(0.4)	316.7	18.4(0.3)	317.1	22.7(0.4)	325.1	62.9(0.4)
382.6	90.3(1.1)	384.7	76.9(2.1)			318.5	19.3(0.2)	319.9	30.2(0.5)		
384.1	106.6(0.8)	387.5	94.5(2.1)			320.2	25.3(0.1)	322.8	35.3(0.4)		
387.1	122.5(1.9)	390.8	106.6(3.4)			322.1	31.1(0.2)	323.6	37.7(0.3)		
389.9	140.8(1.8)					323.3	36.6(0.3)	326.7	52.3(0.2)		
391.4	141.4(1.5)					324.9	36.9(0.3)				
						327.1	39.8(0.3)				
						330.2	60.0(0.4)				
						332.0	61.1(0.3)				

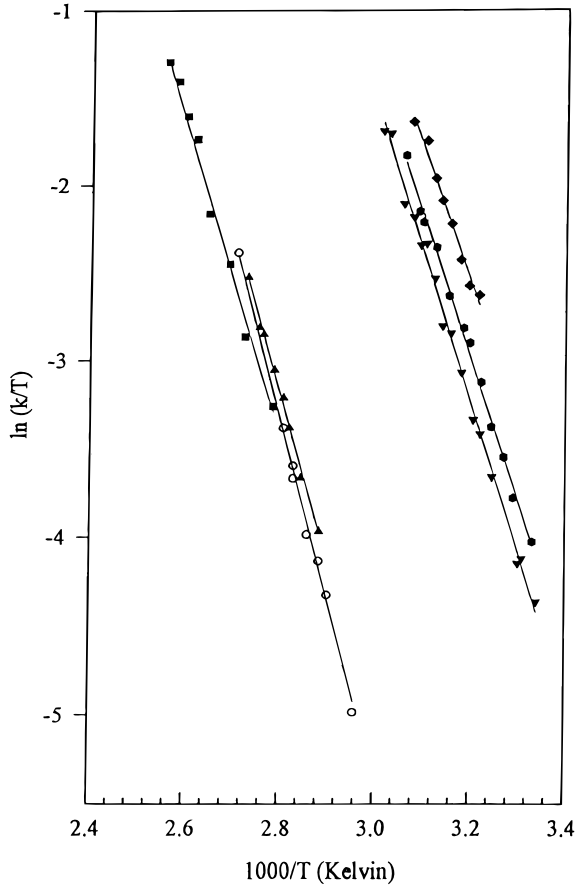

Figure 1. Eyring plots of gas-phase exchange rate constants for asymmetrically substituted formamides and trifluoroacetamides: (○) MPF, (■) MBF, (▲) MIF, (▼) MPTFA, (●) MBTFA, (◆) MITFA.

oxygen) and anti (*N*-methyl group anti to carbonyl oxygen). The observation of separate signals at slow exchange for alkyl protons attached to nitrogen is due to the magnetic anisotropy of the amide group.[4,18,19]

The *N*-methyl protons syn to the carbonyl oxygen experience greater shielding and therefore resonate at higher field than the *N*-methyl protons anti to the carbonyl oxygen in formamide and trifluoroacetamide systems.[19] Conversely, the methylene and methine protons syn to the carbonyl oxygen are observed to resonate at lower field relative to the anti signals. This is consistent with previous reports by Stewart and Siddall,[4] Paulsen and Todt,[19] and LaPlanche and Rogers.[21] The inequality of syn and anti coupling constants also provides conformational information.[4] The long-range J_{H-H} and J_{H-F} coupling constants in *N*-methylalkylformamides and *N*-methyl alkyltrifluoroacetamides are typically larger when the *N*-methyl group is syn to the carbonyl oxygen in formamide systems and anti to the carbonyl oxygen in trifluoroacetamide systems.[15,20,21] The J_{H-F} coupling constants in the present study are smaller than those reported by Suarez et al.[14] This finding is consistent with the previously reported solvent dependence of these coupling constants.[23] Long-range coupling is not seen in any of the gaseous formamide systems, and conformer assignments are determined by comparative analysis with the corresponding liquid system assuming that the relative positions of the resonances are not reversed.

Conformer stability and preference are investigated through analysis of the Gibbs free energy difference, $\Delta G°$, and percentage of preferred conformation. The experimental formamide $\Delta G°$'s (syn−anti) are observed to be small and negative in the gaseous and solution-phase systems and small and positive for the corresponding trifluoroacetamides. It is interesting to note that, in comparison to *N*-methylformamide and other mono-N-substituted alkylamides, *N,N*-asymmetric amides do not exhibit a significant conformational preference.[20−22]

TABLE 2: Conformer Free Energy Differences (cal mol^{-1}) and Percentage of Preferred Conformation

			percentage of syn conformer[b]	
	ΔG^0_{gas}[a]	ΔG^0_{liq}[a]	gas	liquid
MEF[c]	−78(11)	−235(8)	56	73
MPF	−83(14)	−256(17)	55	68
MBF	−80(14)	−242(7)	56	67
MIF	−91(13)	−273(6)	57	69
METFA[c]	204(49)	27(25)	29	48
MPTFA	178(24)	51(42)	32	46
MBTFA	191(53)	77(88)	32	43
MITFA	218(29)	102(32)	30	39

[a] $\Delta G° = G^0_{syn} - G^0_{anti}$. [b] The percentages are reported at 298 K due to the temperature dependence of the populations. [c] Reference 14. Populations have been calculated from reported $\Delta G°$ values.

TABLE 3: Activation Parameters for Gaseous and Solution Phase (1 mol % TClE) MPF, MBF, MIF, MPTFA, MBTFA, and MITFA

	$\Delta G^‡_{298}$ (kcal mol^{-1})		$\Delta H^‡$ (kcal mol^{-1})		$\Delta S^‡$ (cal mol^{-1} K^{-1})	
	gas	liquid	gas	liquid	gas	liquid
MPF	19.4(0.1)	20.3(0.1)	19.5(2.2)	18.5(3.0)	0.3(8.6)	−6.0(9.2)
MBF	19.3(0.1)	20.1(0.1)	19.2(1.6)	18.3(0.3)	−0.3(4.7)	−6.4(0.2)
MIF	19.1(0.1)	19.9(0.1)	18.8(1.1)	18.3(1.8)	−1.0(2.5)	−5.4(5.5)
MPTFA	16.8(0.1)	19.1(0.1)	16.8(1.9)	20.1(1.6)	0.2(8.7)	3.3(5.1)
MBTFA	16.6(0.1)	19.0(0.1)	16.0(0.7)	20.1(2.0)	−1.8(1.2)	3.7(7.4)
MITFA	16.3(0.1)	18.2(0.1)	15.2(1.3)	17.5(1.7)	−3.7(4.4)	−2.3(5.6)

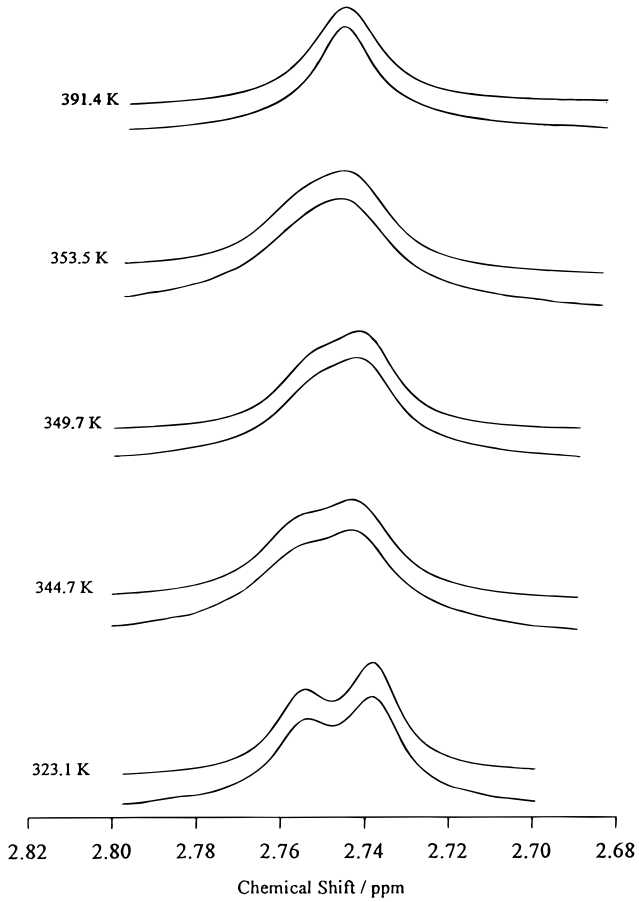

Figure 2. Temperature dependence of the *N*-methyl ^{1}H resonances in gaseous MPF at 300 MHz. The top and bottom traces correspond to calculated and experimental spectra.

***N*-Methyl-*N*-propylformamide.** The slow exchange spectra of gaseous *N*-methyl-*N*-propylformamide (MPF) consist of a triplet (J = 6.71 Hz) at 0.89 ppm, a weak multiplet at 1.56 ppm, two *N*-methyl resonances (singlets) centered at 2.78 ppm with a limiting chemical shift separation of 0.02 ppm ($\Delta\nu$ = 6.00 Hz in a 7.05 T magnetic field), and two methylene triplets (J = 6.71 Hz) centered at 3.20 ppm ($\Delta\nu$ = 59.71 Hz), all downfield from gaseous TMS (δ = 0 ppm). Two formyl proton singlet resonances were observed centered at 7.95 ppm ($\Delta\nu$ = 30.01 Hz). The limiting chemical shift differences are consistently larger for MPF compared to those for *N*-ethyl-*N*-methylformamide.[14] This is the first time both *N*-methyl conformer resonances have been observed in a gaseous formamide system. Previous studies of gaseous *N*-ethyl-*N*-methylformamide[14] and *N*,*N*-dimethylformamide[24] report the *N*-methyl resonances to be isochronic. No temperature dependence of the chemical shifts was observed throughout the slow exchange region. Exchange broadened spectra of the *N*-methyl resonances were obtained over a temperature range of 338.1−353.5 K and 353.5−391.4 K for the methylene resonances. Figure 2 shows the experimental and calculated gas-phase variable temperature ^{1}H spectra of the *N*-methyl resonances.

Additionally, solution-phase exchange data were obtained for a 1 mol % solution in TClE. The slow exchange spectra consist of a triplet (J = 6.71 Hz) centered at 0.88 ppm, a sextet centered at 1.54 ppm, two *N*-methyl singlets centered at 2.85 ppm ($\Delta\nu$ = 21.97 Hz), two methylene triplets (J = 7.33 Hz) centered at 3.16 ppm ($\Delta\nu$ = 28.68 Hz), and a single formyl resonance at 7.97 ppm, downfield from gaseous TMS. The chemical shifts showed a temperature dependence of 0.305(0.082) ppb K^{-1} to higher field for the lower field *N*-methyl resonances and 0.037-(0.069) ppb K^{-1} to higher field for the higher field *N*-methyl resonances. Exchange data were obtained for the *N*-methyl resonances from 386.7 to 405.4 K.

***N*-Butyl-*N*-methylformamide.** The slow exchange spectra of *N*-butyl-*N*-methylformamide (MBF) consist of a triplet (J = 6.71 Hz) at 0.97 ppm, two weak multiplet signals centered at 1.36 and 1.54 ppm, two *N*-methyl singlet resonances centered 2.79 ppm ($\Delta\nu$ = 23.19 Hz), two methylene triplets (J = 5.5 Hz) centered at 3.25 ppm ($\Delta\nu$ = 62.71 Hz), and a singlet formyl resonance centered at 8.01 ppm. No temperature dependence was observed for the chemical shifts throughout the slow exchange region. Exchange broadened spectra were obtained for the methylene resonances from 350.4 to 390.8 K.

The solution-phase slow exchange spectra consist of a triplet (J = 6.71 Hz) at 0.92 ppm, a sextet at 1.29 ppm, a quintet at 1.49 ppm, two singlet *N*-methyl resonances centered at 2.85 ppm ($\Delta\nu$ = 23.19 Hz), and two methylene triplets (J = 6.71 Hz) centered at 3.24 ppm ($\Delta\nu$ = 26.25 Hz). Two formyl singlet resonances were observed centered at 7.97 ppm ($\Delta\nu$ = 3.05 Hz). Solution-phase chemical shifts of the MBF *N*-methyl protons used for line-shape analysis showed a small temperature dependence of 0.460(0.081) ppb K^{-1} to higher field for both the high and low field resonances. Exchange rate data were acquired for the *N*-methyl resonances from 385.6 to 402.1 K.

***N*-Isopropyl-*N*-methylformamide.** The slow exchange spectra of *N*-isopropyl-*N*-methylformamide (MIF) consist of a pair of doublets (J = 6.11 Hz) centered at 1.14 ppm with a limiting chemical shift separation of 20.14 Hz, a singlet *N*-methyl resonance at 2.71 ppm, two methine multiplets centered at 3.72 ppm ($\Delta\nu$ = 47.60 Hz), and two formyl singlet resonances centered at 8.02 ppm ($\Delta\nu$ = 37.23 Hz), downfield from gaseous TMS. No discernible temperature dependence was observed. The exchange rate data were acquired for the isopropyl methyl resonances from 346.9 to 366.1 K.

The solution-phase slow exchange spectra of MIF in 1 mol % TClE consist of two doublets (J = 6.71 Hz) centered at 1.16 ppm ($\Delta\nu$ = 25.03 Hz), two *N*-methyl singlets centered at 2.76 ppm ($\Delta\nu$ = 11.6 Hz), two methine septets centered at 4.16 ppm ($\Delta\nu$ = 248.41 Hz), and two formyl singlet resonances centered at 8.01 ppm ($\Delta\nu$ = 43.95 Hz). A temperature dependence of 0.580(0.035) ppb K^{-1} to higher field for both high and low field resonances was again observed for the solution-phase *N*-methyl resonances. Exchange broadened spectra were obtained from 375.5 to 385.1 K.

***N*-Methyl-*N*-propyltrifluoroacetamide.** The slow exchange spectra of gaseous *N*-methyl-*N*-propyltrifluoroacetamide (MPTFA) consist of a triplet (J = 6.71 Hz) at 0.94 ppm, a sextet at 1.65 ppm, two *N*-methyl resonances centered at 2.99 ppm ($\Delta\nu$ = 37.23 Hz), and a broadened methylene multiplet at 3.38 ppm. The lower field *N*-methyl group was resolved into a quartet (J = 1.22 Hz). The splitting of the low field group was determined to be caused by long-range fluorine coupling. The exchange broadened spectra for the *N*-methyl resonances were obtained over the temperature range 299.4−332.0 K.

The solution-phase slow exchange ^{1}H spectra of MPTFA (1 mol % TClE) consist of a triplet (J = 6.71 Hz) at 0.911 ppm, a sextet at 1.62 ppm, two *N*-methyl resonances (low field is quartet J = 1.22 Hz, high field is broadened singlet) at 2.98 and 3.08 ppm ($\Delta\nu$ = 28.51 Hz), and two methylene resonances at 3.33 ppm (high field signal appears to be slightly broadened) and 3.38 ppm ($\Delta\nu$ = 14.40 Hz). The broadening of the high field methylene group is consistent with unresolved long-range fluorine coupling. Exchange data for the *N*-methyl resonances

were collected from 347.7 to 355.4 K. The fluorine coupling was included in the fitting of these liquid spectra. No evidence of any temperature dependence was observed for the gaseous and solution systems.

***N*-Butyl-*N*-methyltrifluoroacetamide.** The slow exchange spectra of *N*-butyl-*N*-methyltrifluoroacetamide (MBTFA) consist of a triplet ($J = 6.71$ Hz) at 0.98 ppm, two weak multiplets at 1.37 and 1.60 ppm, two *N*-methyl singlets centered at 2.99 ppm ($\Delta\nu = 35.40$ Hz), and a weak broadened methylene resonance at 3.43 ppm, downfield from gaseous TMS. Fluorine coupling was again observed for the *N*-methyl resonances. Exchange data were acquired from 300.2 to 326.7 K for the *N*-methyl resonances.

The solution-phase slow exchange spectra of MBTFA (1 mol % TClE) consist of a triplet ($J = 6.71$ Hz) at 0.94 ppm, a sextet at 1.32 ppm, a quintet at 1.55 ppm, two *N*-methyl resonances (high field is broadened singlet, low field is quartet: $J = 1.22$ Hz) centered at 3.04 ppm ($\Delta\nu = 28.07$ Hz), and a broadened methylene multiplet at 3.38 ppm. *N*-Methyl exchange rate data were acquired from 351.5 to 369.5 K. Again, fitting of the data was accomplished with inclusion of the long-range fluorine coupling, and no temperature dependence was observed for the chemical shifts.

***N*-Isopropyl-*N*-methyltrifluoroacetamide.** The slow exchange ^{1}H spectra of gaseous *N*-isopropyl-*N*-methyltrifluoroacetamide (MITFA) consist of a pair of doublets ($J = 6.71$ Hz) centered at 1.18 ppm ($\Delta\nu = 19.53$ Hz), two *N*-methyl resonances centered at 2.88 ppm ($\Delta\nu = 29.30$ Hz), and two weak methine multiplets centered at 4.56 ppm ($\Delta\nu = 131.84$ Hz). Again, splitting of the low field *N*-methyl group and broadening of the high field methine resonance due to long-range fluorine coupling was observed. No temperature dependence was observed for the chemical shifts. Exchange rate data for internal rotation were acquired from 310.8 to 325.1 K. Figure 3 shows the experimental and calculated ^{1}H spectra of the *N*-methyl resonances.

The solution-phase slow exchange spectra for MITFA consist of a pair of doublets ($J = 6.71$ Hz) centered at 1.19 ppm ($\Delta\nu = 19.53$ Hz), two *N*-methyl resonances centered at 2.89 ppm ($\Delta\nu = 20.15$ Hz), and two methine septets centered at 4.44 ppm ($\Delta\nu = 147.7$ Hz). The fluorine coupling was again included in the fitting of these spectra. Exchange data were acquired for the *N*-methyl resonances from 347.7 to 355.4 K.

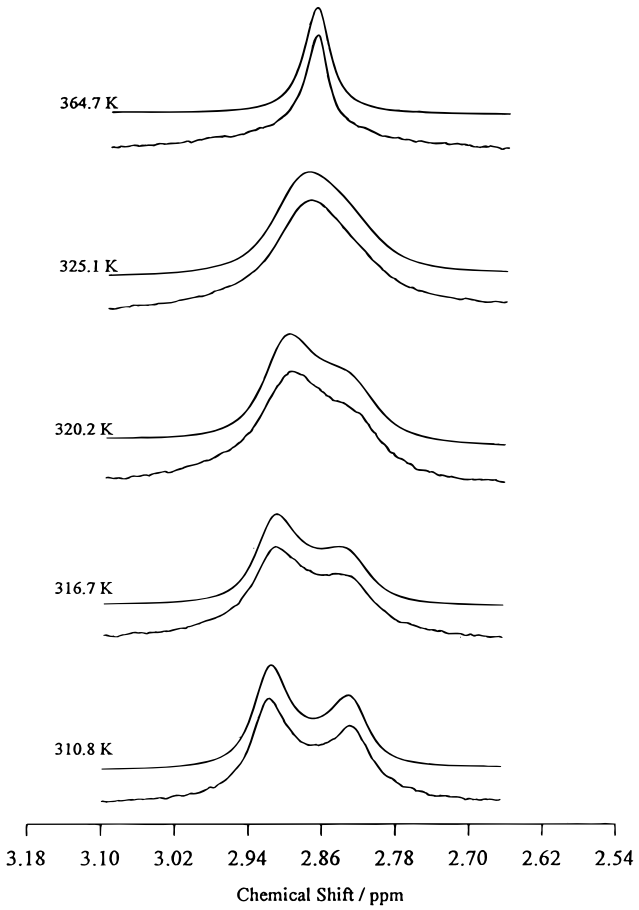

Figure 3. Temperature dependence of the *N*-methyl ^{1}H resonances of gas-phase MITFA at 300 MHz. Top and bottom traces correspond to calculated and experimental spectra.

Discussion

The results of this study confirm the usefulness of gas-phase NMR studies in elucidating conformational preferences and the dependence of the peptide bond rotational barrier on substituent effects. The activation parameters summarized in Table 3 clearly show the dependence of conformational kinetics on medium. Liquid-phase $\Delta G^{\ddagger}_{298}$'s are typically higher (by 1−3 kcal mol^{-1}) than in the gas phase. This increase in the barrier is attributed to the added internal pressure in the liquid and a transition state with greater steric requirements compared to the case of the ground state.[12] Exchange rate constants are also significantly lower in the liquid phase than in the gas, yielding higher activation energies. Due to these solvent perturbations, gas-phase studies are better suited to investigate the subtle intrinsic kinetic and thermodynamic effects of substituents.

The gas-phase rotational barriers summarized in Table 3 of the formamide and trifluoroacetamide systems decrease with increasing substituent bulk. This decrease in barrier height is attributed to the destabilization of the planar ground state. This trend is consistent with previous findings.[12−14] The magnitude, however, of the decline is much smaller in the formamide systems as compared to the trifluoroacetamide systems. The greater decrease in the trifluoroacetamide barriers with increasing substituent bulk indicates greater steric sensitivity in the trifluoroacetamide systems. Replacement of H (1.2 Å) with CF_3 (4.4 Å) produces greater steric repulsion and distorts the planar ground state, resulting in a lower rotational barrier.[25] It should be noted that the differences between MPF and MBF and MPTFA and MBTFA are not as significant as their differences with MIF and MITFA, respectively. This is attributed to much greater steric requirements of the bulky isopropyl group as compared to the straight-chain propyl and butyl groups. The same trend is observed in the liquid systems.

Comparison of our gas-phase formamide and trifluoroacetamide activation barriers with previously reported barriers for symmetric *N*,*N*-disubstituted amides shows that the trifluoroacetamide systems are much more sensitive to increased steric hindrance. The activation barriers to internal rotation for *N*,*N*-dimethyltrifluoroacetamide (16.4 kcal mol^{-1}),[26] *N*,*N*-diethyltrifluoroacetamide (16.1 kcal mol^{-1}),[13] and *N*,*N*-diisopropyltrifluoroacetamide (15.8 kcal mol^{-1})[13] are consistently lower than the barriers for MPTFA and MBTFA. The activation barrier, $\Delta G^{\ddagger}_{298}$, for MITFA is intermediate between the barriers of *N*,*N*-dimethyltrifluoroacetamide and *N*,*N*-diethyltrifluoroacetamide, indicating increased ground-state destabilization with disubstitution of a smaller ethyl alkyl group. The most sterically hindered system, *N*,*N*-diisopropyltrifluoroacetamide, displays the greatest ground-state destabilization with an activation barrier of 15.8 kcal mol^{-1}. The magnitude of the changes in the activation barriers with increased steric requirements in the formamide systems is much less pronounced in comparison to

their trifluoroacetamide counterparts. The activation parameters, in kcal mol^{-1}, for *N*,*N*-dimethylformamide, *N*,*N*-diethylformamide, and *N*,*N*-diisopropylformamide are 19.4,[24]19.6,[12] and 19.0,[12] respectively. We observe no difference in the activation barriers between MPF and *N*,*N*-dimethylformamide and a minor difference with MBTFA. $\Delta G^{\ddagger}_{298}$ for MIF is lower than the activation barrier for *N*,*N*-diethylformamide and higher than that for *N*,*N*-diisopropylformamide by 0.1 kcal mol^{-1}, demonstrating the weaker influence of substituent bulk on the barrier compared to the trifluoroacetamide systems.

The effect of substituent electronegativity on amide internal rotation barriers has been investigated in both the gas[16] and liquid phases.[15,27−31] The transition state is more affected by carbonyl substituent electronegativity effects because the carbonyl moiety in the transition state is more electrophilic than in the ground state. In trifluoroacetamides, the repulsive interaction between the positively charged trifluoro carbon and the positively charged carbonyl carbon results in a destabilization of the transition state, which should raise the rotational barrier. Our results show the formamide internal rotation barriers are substantially higher (≈2.5 kcal mol^{-1}) than the corresponding trifluoroacetamide barriers, indicating a much higher degree of ground-state destabilization due to steric interactions in the trifluoroacetamides. Close inspection reveals that the most bulky substituent (the isopropyl group) serves to lower the liquid internal rotational barriers to an even greater extent.

Table 2 shows that in the gas phase the population of the syn conformer is ca. 55% for the formamides studied and ca. 30% for the trifluoroacetamides studied. The percentage is not very sensitive to the length of the alkyl chain or whether the substituent is a straight-chain alkyl group or an isopropyl group. The lower population of the syn conformer in the trifluoroacetamides compared to the formamides indicates the presence of a destabilizing steric interaction between the CF_3 group and the alkyl substituent. The temperature-dependent population data obtained in the present study were limited by low sample vapor pressure and were not adequate to separate the energy differences, $\Delta G°$'s, listed into entropic and enthalpic contributions. The steric destabilization may be caused by either enthalpic factors such as electrostatic repulsion between the alkyl group and the CF_3 group or entropic factors such as increases in internal rotation barriers when the alkyl group is adjacent to the CF_3 group or, more likely, a combination of both factors.

When the formamides listed in Table 2 are dissolved in the relatively nonpolar solvent, TClE, the population of the syn conformer increases to ca. 70% for the formamides and to ca. 45% for the trifluoroacetamides. In both cases this is a ca. 15% increase relative to the gas-phase values. The populations of the syn and anti conformers of the trifluoroacetamides listed in Table 2 were also measured in methanol solutions, and in this more polar solvent the population of the syn conformer is ca. 50%. It is possible that the accessibility of both the polar carbonyl group and the relatively nonpolar alkyl group to stabilizing solvent interactions is greater for the syn conformer and may account for these observations. In the anti conformation, stabilizing electrostatic interactions between the alkyl chains and the carbonyl group can occur, making both groups less available to solvent molecules. This effect is eliminated when the carbonyl and methyl groups are syn, and the syn conformer may be stabilized by solvation by both polar and nonpolar solvent molecules to a greater extent than the anti conformer.

Although the stability and reactivity of liquid amides have been extensively investigated,[11,27,29] the conformational dynamics of gaseous asymmetric systems have not. Solvents clearly influence conformer stability and free energy differences. The differences between gas- and liquid-phase $\Delta G°$'s are significant. The rotational barriers also change with phase, though these effects have been well documented.[12−14,24] The gas-phase rotational barriers are consistently lower than in the liquid phase.

In conclusion, the conformational equilibria and the internal rotation barriers of the asymmetric amides studied are primarily influenced by the nature of the substituent on the carbonyl carbon and by the medium. The conformational equilibria are relatively insensitive to the nature of the alkyl substituent. The rotational barriers, however, are influenced by the alkyl substituent, yielding smaller $\Delta G^{\ddagger}_{298}$ values with increased substituent bulk.

Acknowledgment. We are pleased to acknowledge the National Science Foundation (CHE 93-21079) for support of this research. We would also like to thank Robert K. Bohn for the gift of the *N*-methyl-*N*-propylformamide.

References and Notes

(1) Kyte, J. *Mechanism in Protein Chemistry*; Garland: New York, 1995.
(2) Lehninger, A. L.; Nelson, D. L.; Cox, M. M. *Principles of Biochemistry*; Worth: New York, 1993.
(3) Wiberg, K. B.; Hadad, C. M.; Rablen, P. R.; Cioslowski, J. *J. Am. Chem. Soc*. **1992**, *114*, 8644.
(4) Stewart, W. E.; Siddall, T. H., III. *Chem. Rev*. **1970**, *70*,517.
(5) Jackman, L. M. In *Dynamic Nuclear Magnetic Resonance Spectroscopy*; Jackman, L. M., Cotton, F. A., Eds.; Academic Press: New York, 1975; pp 203−252 and references therein.
(6) Mirkin, N. G.; Krimm, S. *J. Am Chem. Soc*. **1991**, *113*, 9742.
(7) Sapse, A. M.; Mallah-Levy, L.; Daniels, S. B.; Erickson, B. W. *J. Am. Chem. Soc*. **1987**, *109*, 3526.
(8) Duffy, E. M.; Severance, D. L.; Jorgenson, W. L. *J. Am. Chem. Soc*. **1992**, *114*, 75.
(9) Stein, S. E. *J. Am. Chem. Soc*. **1981**, *103*, 5685.
(10) Kang, Y. K.; No, K. T.; Scheraga, H. A. *J. Phys. Chem*. **1996**, *100*, 15588.
(11) Jorgenson, W. L.; Gao, J. *J. Am. Chem. Soc*. **1988**, *110*, 4212.
(12) LeMaster, C. B.; True, N. S. *J. Phys. Chem*. **1989**, *93*, 1307.
(13) Suarez, C.; LeMaster, C. B.; LeMaster, C. L.; Tafazzoli, M.; True, N. S. *J. Phys. Chem*. **1990**, *94*, 6679.
(14) Suarez, C.; True, N. S. *J. Phys. Chem*. **1995**, *99*, 8170.
(15) LaPlanche, L. A.; Rogers, M. T. *J. Am. Chem. Soc*. **1963**, *85*, 3728.
(16) Ross, B. D.; Wong, L. T.; True, N. S. *J. Phys. Chem*. **1985**, *89*, 836.
(17) (a) Stephenson, D. S.; Binsch, G. Program No. 365. (b) LeMaster, C. B.; LeMaster, C. L.; True, N. S. Programs No. 569 and QCMP059. Quantum Chemistry Program Exchange, Indiana University, Bloomington, IN 47405.
(18) Narasimhan, P. T.; Rogers, M. T. *J. Phys. Chem*. **1959**, *63*, 1388.
(19) Paulsen, H.; Todt, K. *Agnew. Chem., Int. Ed. Engl*. **1966**, *5*, 899.
(20) Neuman, R. C.; Young, L. B. *J. Phys. Chem*. **1965**, *69*, 1777.
(21) LaPlanche, L. A.; Rogers, M. T. *J. Am. Chem. Soc*. **1964**, *86*, 337.
(22) Fantoni, A. C.; Caminati, W. *J. Chem Soc., Faraday Trans*. **1996**, *92*, 343.
(23) Fraenkel, G.; Franconi, C. *J. Am. Chem Soc*. **1960**, *82*, 4478.
(24) Ross, B. D.; True, N. S. *J. Am. Chem. Soc*. **1984**, *106*, 2451.
(25) The diameter of the CF_3 group is 4.4 Å and of the CH_3 3.8 Å as estimated from AMPAC results using the AMI Hamiltonian. Program No. 506, Quantum Chemistry Program Exchange, Indiana University, Bloomington, IN 47405.
(26) Ross, B. D.; True, N. S.; Decker, D. L. *J. Phys. Chem*. **1983**, *87*, 89.
(27) Graham, L. L. *Org. Magn. Reson*. **1972**, *4*, 335.
(28) Perrin, C. L.; Dwyer, T. J.; Rebek, J., Jr.; Duff, R. J. *J. Am. Chem. Soc*. **1990**, *112*, 3122.
(29) Spencer, J. N. *J. Chem. Phys*. **1981**, *85*, 1236.
(30) Allan, E. A.; Hobson, R. F.; Reeves, L. W.; Shaw, K. N. *J. Am. Chem. Soc*. **1972**, *94*, 6604.
(31) Reeves, L. W.; Shaw, K. N. *Can. J. Chem*. **1971**, *49*, 3672.